

v-ATPase V₀ subunit d2-deficient mice exhibit impaired osteoclast fusion and increased bone formation

Seoung-Hoon Lee¹, Jaerang Rho^{1,6}, Daewon Jeong^{1,6}, Jai-Yoon Sul², Taesoo Kim¹, Nacksung Kim^{1,6}, Ju-Seob Kang^{1,6}, Takeshi Miyamoto³, Toshio Suda³, Sun-Kyeong Lee⁴, Robert J Pignolo⁵, Boguslawa Koczon-Jaremko⁴, Joseph Lorenzo⁴ & Yongwon Choi¹

Matrix-producing osteoblasts and bone-resorbing osteoclasts maintain bone homeostasis. Osteoclasts are multinucleated, giant cells of hematopoietic origin formed by the fusion of mononuclear pre-osteoclasts derived from myeloid cells^{1,2}. Fusion-mediated giant cell formation is critical for osteoclast maturation; without it, bone resorption is inefficient^{2,3}. To understand how osteoclasts differ from other myeloid lineage cells, we previously compared global mRNA expression patterns in these cells and identified genes of unknown function predominantly expressed in osteoclasts, one of which is the d2 isoform of vacuolar (H⁺) ATPase (v-ATPase) V₀ domain (*Atp6v0d2*)^{4–7}. Here we show that inactivation of *Atp6v0d2* in mice results in markedly increased bone mass due to defective osteoclasts and enhanced bone formation. *Atp6v0d2* deficiency did not affect differentiation or the v-ATPase activity of osteoclasts. Rather, *Atp6v0d2* was required for efficient pre-osteoclast fusion. Increased bone formation was probably due to osteoblast-extrinsic factors, as *Atp6v0d2* was not expressed in osteoblasts and their differentiation *ex vivo* was not altered in the absence of *Atp6v0d2*. Our results identify *Atp6v0d2* as a regulator of osteoclast fusion and bone formation, and provide genetic data showing that it is possible to simultaneously inhibit osteoclast maturation and stimulate bone formation by therapeutically targeting the function of a single gene.

Mature osteoclasts possess properties not found in other monocyte-derived cells. To understand how osteoclasts differ from macrophages or dendritic cells, we previously identified a cDNA fragment for a new v-ATPase d subunit homolog, which is highly enriched in osteoclasts⁷. Full-length cDNA analysis has shown that it encodes a protein identical to the recently reported v-ATPase subunit d2 (*Atp6v0d2*)^{4–6}, except for one amino acid residue. In contrast to previous reports, we found that the *Atp6v0d2* gene produces two transcripts, ~2.5 kb

and ~1.4 kb in length, which differ only in the 3' untranslated region. *Atp6v0d2* expression is highly upregulated during osteoclast differentiation and is most abundant in mature osteoclasts (Supplementary Fig. 1 online).

Multiple isoforms of v-ATPase subunits have been identified that show distinct cell type- and tissue-specific expressions, and these isoforms are proposed to account for the diverse physiological properties of the ubiquitous v-ATPases among these distinct cell types^{8,9}. Two isoforms of the v-ATPase V₀ subunit d, d1 and d2, have been identified in mice and humans. Although structurally homologous to *Atp6v0d1*, the functional importance of *Atp6v0d2* was unknown^{4–7}. To define *Atp6v0d2* function, we generated *Atp6v0d2*^{−/−} mice (Supplementary Fig. 1). Northern and western blot analysis confirmed the lack of *Atp6v0d2* mRNA and protein expression (Fig. 1a). *Atp6v0d2*^{−/−} mice were born at the expected mendelian ratio and exhibited normal growth rates, without overt defects. The level of *Atp6v0d2* mRNA was extremely low: at least 10 times lower than that of d1 subunit in osteoclasts, and at least 200 times lower than d1 in other tissues (Supplementary Fig. 1). Consistently, the brain, heart, lung, liver, spleen and intestine appeared normal in *Atp6v0d2*^{−/−} mice (data not shown). Additionally, the kidneys of *Atp6v0d2*^{−/−} mice showed no histological defects, and v-ATPase function and subsequent regulation of urinary pH were normal (Supplementary Fig. 2 online).

To determine the impact of *Atp6v0d2* deficiency on bone, we performed high-resolution microcomputed tomography (μCT) studies, which revealed marked increases in bone mass and micromerit decreases in bone marrow cavity space in the absence of *Atp6v0d2* (Fig. 1b and Supplementary Table 1 online). Bone sections stained for tartrate-resistant acid phosphatase (TRAP) revealed that the number of TRAP⁺ cells was comparable in the bones of *Atp6v0d2*^{−/−} mice and control littermates. However, there was a substantial reduction in osteoclast surface extent and the number of multinucleated TRAP⁺ cells and a slight increase in the number of mononuclear

¹Department of Pathology and Laboratory Medicine, and ²Department of Neuroscience, University of Pennsylvania School of Medicine, Philadelphia, Pennsylvania 19104, USA. ³Department of Cell Differentiation and Orthopedic Surgery, School of Medicine, Keio University, 35 Shinano-machi, Shinjuku-ku, Tokyo 160-8582, Japan. ⁴Division of Endocrinology, Department of Medicine, MC-5456, University of Connecticut Health Center, Farmington, Connecticut 06030, USA. ⁵Department of Medicine, University of Pennsylvania School of Medicine, Philadelphia, Pennsylvania 19104, USA. ⁶Present addresses: Department of Microbiology, Chungnam National University, Daejeon 305-764, Korea (J.R.), Department of Microbiology, Yeungnam University College of Medicine, 317-1 Daemyungdong, Namgu, Daegu 705-717, Korea (D.J.), Medical Research Center for Gene Regulation, Chonnam National University Medical School, Gwangju 501-746, Korea (N.K.) and Department of Pharmacology, College of Medicine and Institute of Biomedical Science, Hanyang University, Seoul 133-791, Korea (J.-S.K.). Correspondence should be addressed to Y.C. (ychoi3@mail.med.upenn.edu).

Received 4 October; accepted 31 October; published online 26 November 2006; doi:10.1038/nm1514

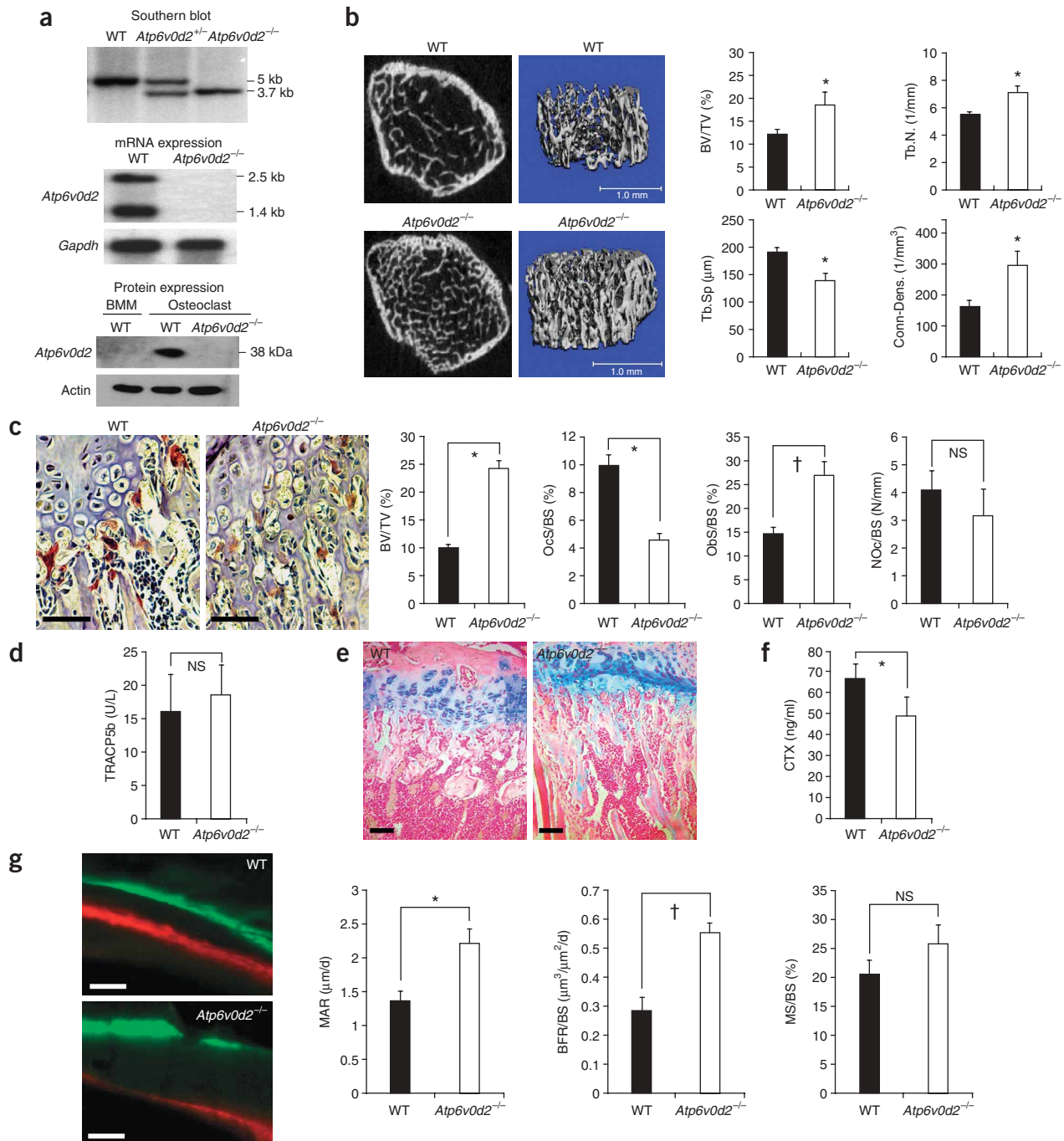


Figure 1 Deletion of *Atp6v0d2* leads to defective osteoclasts and increased bone formation. **(a)** Top, confirmation of *Atp6v0d2* deletion by Southern blot. Genomic DNA from *Atp6v0d2*^{+/+} (wild-type, WT), *Atp6v0d2*^{+/-} and *Atp6v0d2*^{-/-} mice was isolated, digested with *SphI*, and probed with "Probe 1" (see **Supplementary Fig. 1**). Wild-type and null alleles were ~ 5 kb and 3.7 kb, respectively, in length. Middle, *Atp6v0d2* RNA expression in osteoclasts. Bottom, *Atp6v0d2* protein expression. Whole-cell extracts from wild-type osteoclast precursors (BMM) and from wild-type or *Atp6v0d2*^{-/-} osteoclasts were examined with rabbit *Atp6v0d2*-specific polyclonal antibody by western blot analysis. **(b)** Tibias, femurs and vertebra from 8- to 10-week-old control, wild-type and *Atp6v0d2*^{-/-} mice were examined by μCT. Two-dimensional (left) and three-dimensional (right) reconstruction of femurs revealed increased bone mass in *Atp6v0d2*^{-/-} mice compared with control littermates. Histograms represent three-dimensional trabecular structural parameters in the secondary spongiosa of the distal femur: bone volume fraction (BV/TV), trabecular number (Tb.N), trabecular spacing (Tb.Sp) and trabecular connectivity density (Conn-Dens). **P* < 0.05. Data represent mean ± s.e.m. *n* = 6–8. **(c)** Static histomorphometry analysis of femurs from 6- to 7-week-old *Atp6v0d2*^{-/-} mice and control littermates: bone volume (BV/TV), osteoclast surface per bone surface (OcS/BS), osteoblast surface per bone surface (Obs/BS) and osteoclast number per bone surface (NOc/BS). **P* < 0.005, †*P* < 0.05. Data represent mean ± s.e.m. *n* = 4. **(d)** Serum TRACP5b levels were measured by ELISA. **(e)** Alcian blue staining on femurs from 6- to 7-week-old *Atp6v0d2*^{-/-} mice and control littermates. **(f)** Serum type 1 collagen cross-linked telopeptide (CTX) measured by ELISA. **P* < 0.05. **(g)** Dynamic histomorphometry analysis of femurs from 6- to 7-week-old *Atp6v0d2*^{-/-} mice and control littermates: mineral apposition rate (MAR), bone formation rate (trabecular bone surface) (BFR/BS) and mineralizing surface (MS/BS). **P* < 0.05, †*P* < 0.01. Data represent mean ± s.e.m. *n* = 4–5. Scale bar, 100 μm. For values other than those presented here, see **Supplementary Table 1**. NS, not significant.

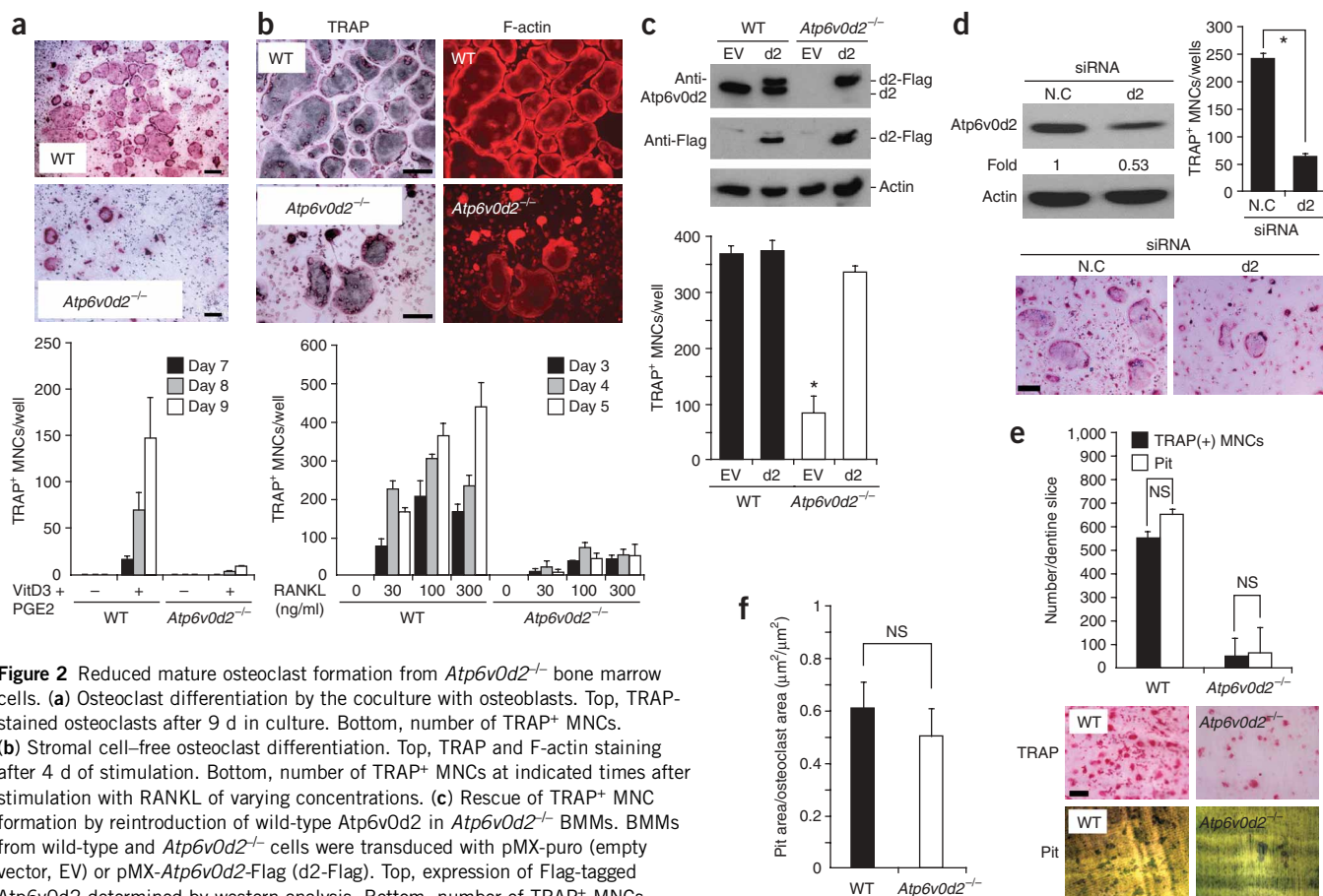


Figure 2 Reduced mature osteoclast formation from *Atp6v0d2*^{-/-} bone marrow cells. **(a)** Osteoclast differentiation by the coculture with osteoblasts. Top, TRAP-stained osteoclasts after 9 d in culture. Bottom, number of TRAP⁺ MNCs. **(b)** Stromal cell-free osteoclast differentiation. Top, TRAP and F-actin staining after 4 d of stimulation. Bottom, number of TRAP⁺ MNCs at indicated times after stimulation with RANKL of varying concentrations. **(c)** Rescue of TRAP⁺ MNC formation by reintroduction of wild-type *Atp6v0d2* in *Atp6v0d2*^{-/-} BMMs. BMMs from wild-type and *Atp6v0d2*^{-/-} cells were transduced with pMX-puro (empty vector, EV) or pMX-*Atp6v0d2*-Flag (d2-Flag). Top, expression of Flag-tagged *Atp6v0d2* determined by western analysis. Bottom, number of TRAP⁺ MNCs. **(d)** Reduction of TRAP⁺ MNC formation by siRNA-mediated knockdown of wild-type *Atp6v0d2*. BMMs from wild-type mice were transfected with control siRNA (N.C.) or siRNA for *Atp6v0d2* (d2). Top left, expression of *Atp6v0d2* protein. Top right, number of TRAP⁺ MNCs. Bottom, TRAP-stained osteoclasts. **(e)** Bone-resorption pits from wild-type and *Atp6v0d2*^{-/-} osteoclasts. Osteoclasts were made by culturing osteoclast precursors with RANKL and M-CSF (BMM) on dentine slices. Data represent mean \pm s.d. and are representative of at least three experiments. **(f)** Osteoclasts were generated on dentine slices, and the mean resorption area was determined using the Via-160 video image maker measurement system (Boeckeler Instruments). **P* < 0.01. Scale bar, 200 μ m. WT, wild type. NS, not significant.

TRAP⁺ cells in *Atp6v0d2*^{-/-} mice compared to control littermates (Fig. 1c and Supplementary Table 1). These results suggest that osteoclast maturation, not differentiation, might be affected in *Atp6v0d2*^{-/-} mice. Consistently, serum TRACP5b levels, a measure of early commitment to the osteoclast lineage, were comparable in *Atp6v0d2*^{-/-} mice and control littermates (Fig. 1d). However, *Atp6v0d2*^{-/-} mice had increased cartilage remnants, a characteristic of osteopetrosis due to defective resorption, and reduced serum type 1 collagen cross-linked C-terminal telopeptide, a direct measure of resorptive activity (Fig. 1e,f). These results indicate that increased bone mass in *Atp6v0d2*^{-/-} mice is due, in part, to reduced bone resorption.

Atp6v0d2^{-/-} mice also exhibited a marked increase in osteoblasts and bone formation rate (Fig. 1c,g and Supplementary Table 1). However, *Atp6v0d2* was not detected in osteoblasts. In addition, *Atp6v0d2* deletion did not affect osteoblast differentiation or the expression of osteoblast differentiation markers such as *Dlx5*, *Sp7* (*Osx*) or *Runx2* *in vitro* (Supplementary Fig. 2). Thus, increased osteoblast activity in *Atp6v0d2*^{-/-} mice is probably due to osteoblast-extrinsic factors, possibly produced by mutant osteoclasts or their immediate precursors.

To examine osteoclast defects in *Atp6v0d2*^{-/-} mice, we next used two standard *in vitro* osteoclast culture methods^{7,10,11}: coculture of

primary osteoblasts with bone marrow monocyte precursors (BMMs), or stromal cell-free BMM cultures with receptor activator of NF- κ B ligand (RANKL) and macrophage colony-stimulating factor (M-CSF). In both methods, osteoclasts, identified as TRAP⁺ cells, were generated from BMMs of *Atp6v0d2*^{-/-} mice (Fig. 2a,b). However, most *Atp6v0d2*^{-/-} osteoclasts were much smaller than wild-type osteoclasts. The formation of large (> 100 μ m) osteoclasts containing more than five nuclei and an actin ring was greatly diminished in the absence of *Atp6v0d2* (Fig. 2a,b). This defect was not due to the failure of *Atp6v0d2*^{-/-} osteoblasts to support osteoclast differentiation (Supplementary Fig. 2); rather, it seemed to result directly from the loss of *Atp6v0d2* in BMMs. Reintroduction of wild-type *Atp6v0d2* into *Atp6v0d2*^{-/-} BMMs restored their ability to become large TRAP⁺ multinucleated cells (MNCs), and, in a complementary approach, *Atp6v0d2* knockdown in wild-type BMMs reduced the formation of TRAP⁺ MNCs (Fig. 2c,d and Supplementary Fig. 2). Although the total number of pits on dentine slices formed by *Atp6v0d2*^{-/-} osteoclasts was markedly reduced (Fig. 2e), which correlates with the degree of reduction in the number of actin ring-positive, large TRAP⁺ MNCs (Fig. 2e), the area of pits formed by the *Atp6v0d2*^{-/-} osteoclasts was similar to that in cells from wild-type mice (Fig. 2f). These results suggest that *Atp6v0d2* regulates the formation of large MNCs, but, once formed, resorption by these cells occurs at a rate

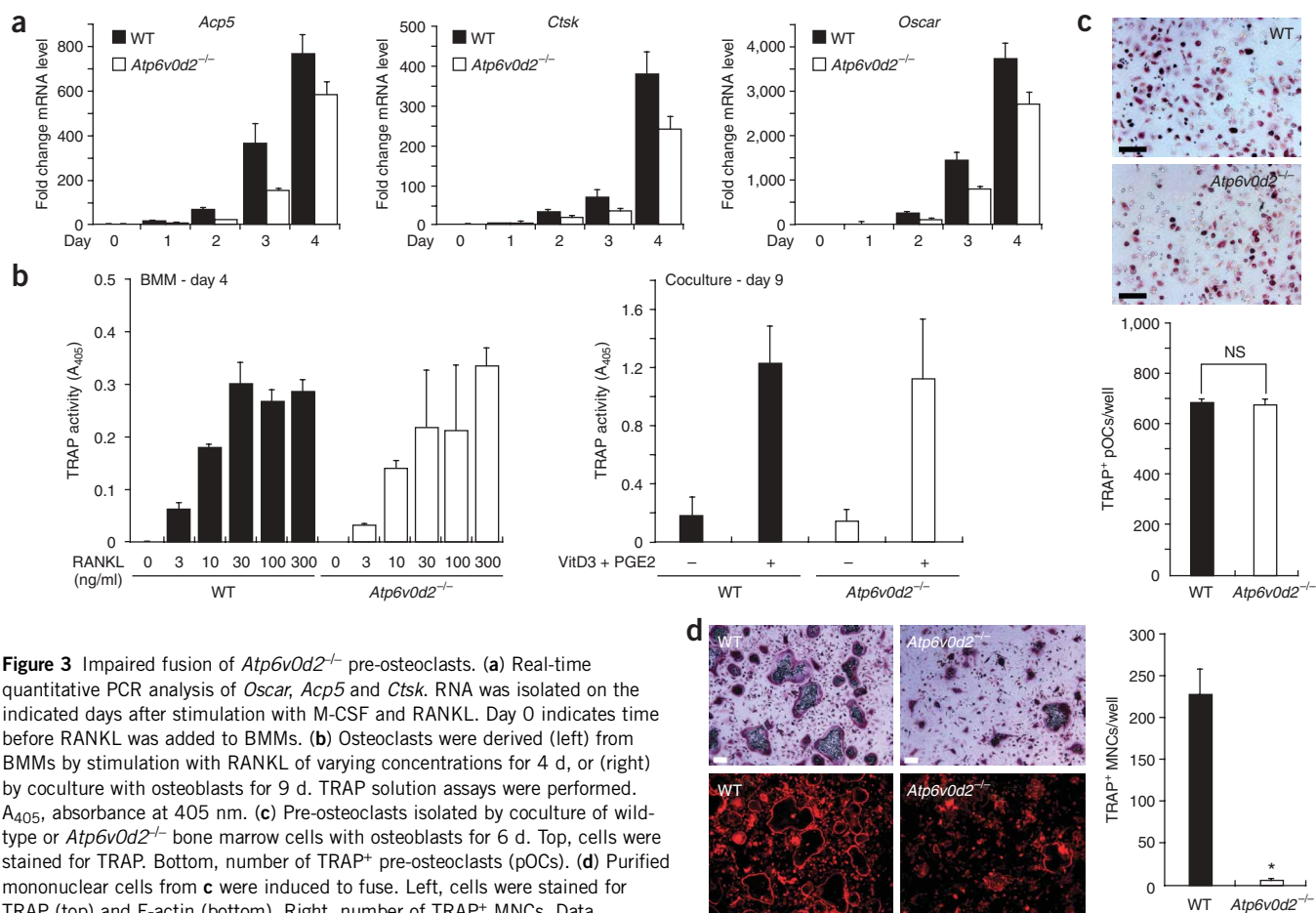


Figure 3 Impaired fusion of *Atp6v0d2*^{-/-} pre-osteoclasts. **(a)** Real-time quantitative PCR analysis of *Oscar*, *Acp5* and *Ctsk*. RNA was isolated on the indicated days after stimulation with M-CSF and RANKL. Day 0 indicates time before RANKL was added to BMMs. **(b)** Osteoclasts were derived (left) from BMMs by stimulation with RANKL of varying concentrations for 4 d, or (right) by coculture with osteoblasts for 9 d. TRAP solution assays were performed. A₄₀₅, absorbance at 405 nm. **(c)** Pre-osteoclasts isolated by coculture of wild-type or *Atp6v0d2*^{-/-} bone marrow cells with osteoblasts for 6 d. Top, cells were stained for TRAP. Bottom, number of TRAP⁺ pre-osteoclasts (pOCs). **(d)** Purified mononuclear cells from **c** were induced to fuse. Left, cells were stained for TRAP (top) and F-actin (bottom). Right, number of TRAP⁺ MNCs. Data represent mean \pm s.d. and are representative of at least three experiments. WT, wild type. NS, not significant. **P* < 0.01. Scale bar, 100 μ m.

equivalent to that in wild-type cells^{2,12}. Indeed, the activity of v-ATPases from *Atp6v0d2*^{-/-} osteoclasts was similar to that of v-ATPases from wild-type cells (Supplementary Fig. 3 online).

The formation of multinucleated mature osteoclasts depends on the fusion of mononuclear pre-osteoclasts. To determine which steps of these processes are affected by *Atp6v0d2* deficiency, we first examined the expression of molecular markers signifying differentiated osteoclasts. mRNA expression levels of the genes encoding osteoclast-associated receptor, cathepsin K and TRAP (*Oscar*, *Ctsk* and *Acp5*) were comparable between *Atp6v0d2*^{-/-} and wild-type osteoclasts (Fig. 3a). Total TRAP activity, accounting for both mono- and multinucleated osteoclasts, was comparable between *Atp6v0d2*^{-/-} and wild-type osteoclast cultures (Fig. 3b), consistent with *in vivo* bone parameters (Fig. 1 and Supplementary Table 1). When the efficiency of mononuclear pre-osteoclast formation was directly measured from BMMs of wild-type littermates and *Atp6v0d2*^{-/-} mice^{10,13}, there were no marked differences (Fig. 3c). Hence, early steps of osteoclast differentiation do not seem to be affected by *Atp6v0d2* deficiency. We next determined whether subsequent cell-cell fusion of pre-osteoclasts was affected by the *Atp6v0d2* deletion by inducing the fusion of purified pre-osteoclasts. When the fusion outcome was measured in terms of the number of large TRAP⁺ MNCs formed, there was substantial reduction in the formation of mature giant osteoclasts in the absence of *Atp6v0d2* (Fig. 3d). Once formed, however, the survival rate of *Atp6v0d2*^{-/-} MNCs was

similar to that of wild-type cells (Supplementary Fig. 3). Thus, *Atp6v0d2* is not involved in the differentiation of BMMs up to TRAP⁺ mononuclear pre-osteoclasts, but it does influence subsequent cell-cell fusion to generate multinucleated mature osteoclasts. This result is consistent with our finding that there was a reduction in the average number of nuclei per TRAP⁺ cell in *Atp6v0d2*^{-/-} mice compared to control littermates (2 ± 0.06 versus 1.38 ± 0.1 ; Supplementary Table 1).

The mechanism regulating cell-cell fusion during osteoclast maturation remains largely unknown. Although many molecules were previously implicated in osteoclast fusion^{3,14,15}, only dendritic cell-specific transmembrane protein (DC-STAMP) has been shown to be critical for osteoclast fusion by genetic studies *in vivo*³. To define the potential mechanism affected by the absence of *Atp6v0d2*, we first examined whether defects in the *Atp6v0d2*^{-/-} pre-osteoclasts are dominant or recessive to wild-type pre-osteoclasts during fusion. When wild-type and *Atp6v0d2*^{-/-} pre-osteoclasts were mixed and then induced to fuse, the formation of large TRAP⁺ MNCs was restored to a level comparable to that in cultures containing only the wild-type pre-osteoclasts, suggesting that wild-type pre-osteoclasts can fuse with *Atp6v0d2*^{-/-} pre-osteoclasts and restore the fusion capacity of *Atp6v0d2*^{-/-} cells (Fig. 4a,b and Supplementary Fig. 3). This ability did not seem to be due to soluble factors produced by wild-type cells, as they could not rescue the defects of *Atp6v0d2*^{-/-} cells in trans-well plates (Supplementary Fig. 3).

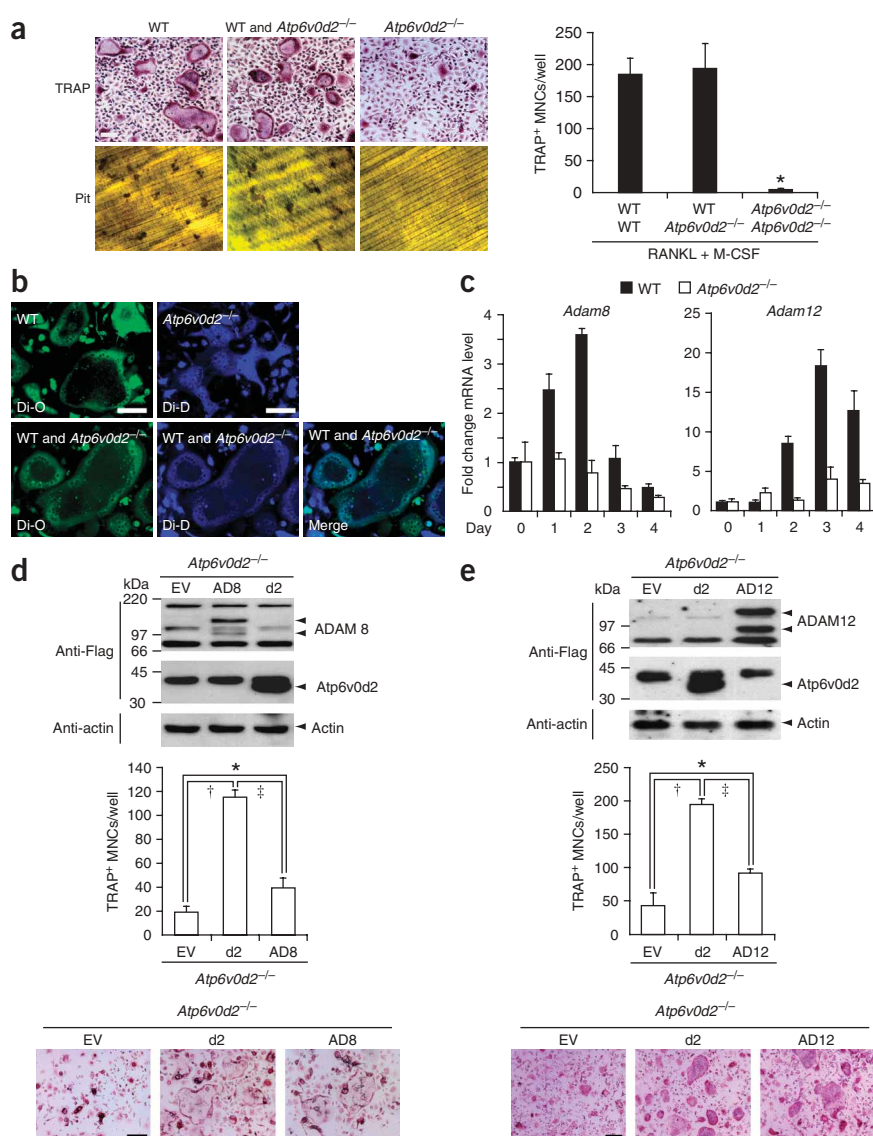


Figure 4 Rescue of cell fusion in *Atp6v0d2*^{-/-} osteoclasts by ADAM8 or ADAM12. **(a)** Pre-osteoclasts from wild-type (WT) and *Atp6v0d2*^{-/-} bone marrow cells were cultured independently or mixed in the presence of M-CSF and RANKL for 24 h. WT, wild type only; WT and *Atp6v0d2*^{-/-}, equal mixture of wild-type and mutant cells; *Atp6v0d2*^{-/-}, mutant cells only. Left, TRAP staining and bone resorption pits. Right, number of TRAP⁺ MNCs. **P* < 0.01. Scale bar, 100 μm. **(b)** For heterotypic fusion, DiO-stained wild-type (WT) and DiD-stained mutant (*Atp6v0d2*^{-/-}) pre-osteoclasts were cultured independently (top) or mixed in equal numbers (bottom) for fusion assays, and examined using fluorescence microscopy. Scale bar, 100 μm. **(c)** *Adam8* (left) and *Adam12* (right) expression during osteoclast differentiation. RNA was isolated from BMMs (day 0) and subsequently treated with M-CSF and RANKL (days 1–4). **(d,e)** Rescue of TRAP⁺ MNC formation by retrovirus-mediated expression of *Atp6v0d2*, ADAM8 or ADAM12 in *Atp6v0d2*^{-/-} BMMs. EV, empty vector; d2, *Atp6v0d2*-Flag; AD8, ADAM8-Flag; AD12, ADAM12-Flag. Expression of Flag-tagged *Atp6v0d2*, ADAM8 (left) or ADAM12 (right) was confirmed by immunoblot analysis using antibody to Flag. TRAP⁺ MNCs were counted as described above. A representative TRAP staining is also shown. Scale bar, 200 μm. Data represent mean ± s.d. and are representative of three experiments. **P* < 0.05, †*P* < 0.01, ‡*P* < 0.02.

MNCs that resorbed bone (Fig. 4d,e). The rescue of *Atp6v0d2*^{-/-} BMMs by ADAM8 or ADAM12 transduction, however, was less efficient (~30–40%) than that by wild-type *Atp6v0d2* transduction (Fig. 4d,e). These results indicate that the increased level of ADAM8 or ADAM12 can partially complement the defective fusion of *Atp6v0d2*^{-/-} osteoclasts.

Our studies provide strong genetic evidence that *Atp6v0d2* is a new factor required for optimal cell-cell fusion. *Atp6v0d2* was recognized previously to be structurally similar to *Atp6v0d1*, but the functional importance of *Atp6v0d2* in v-ATPase activity was not established^{4,5}. Moreover, most of the v-ATPase complexes were shown to be composed of *Atp6v0d1*, even in the nonphysiological conditions allowing *Atp6v0d2* incorporation into v-ATPase complexes⁴. In mature osteoclasts, the level of *Atp6v0d1* expression is much higher (~10 times) than that of *Atp6v0d2*, suggesting that *Atp6v0d2* may not be a critical constituent of v-ATPase complexes in these cells. Although our results do not completely rule out the importance of *Atp6v0d2* for the v-ATPase proton pump, bone resorption, which requires functional v-ATPase proton pumps, was not affected by *Atp6v0d2* deletion. It is thus likely that the primary role of osteoclast-expressed *Atp6v0d2* is as a regulator of fusion. The question of how *Atp6v0d2* regulates cell fusion remains to be answered. It does not seem to directly regulate or interact with ADAM8 or ADAM12, nor does it involve DC-STAMP, RANK or nuclear factor of activated T cells c1 (NFATc1) (Supplementary Figs. 6,7 online). If *Atp6v0d2* assumes an evolutionarily conserved role in regulating cell-cell fusion, its deficiency may also affect the fusion of other cell types. Consistently, cytokine-induced fusion of

Our data suggest that *Atp6v0d2* deficiency most probably causes the reduction of factors necessary for fusion. To investigate this point further, we measured mRNA expression of molecules implicated previously in cell-cell fusion: E-cadherin, DC-STAMP, integrins, Src-family kinases and a disintegrin and metalloprotease domain (ADAM)-family proteins^{3,14,15}. RNA levels of most genes were remarkably similar between wild-type and *Atp6v0d2*^{-/-} cells during the entire course of osteoclast differentiation and maturation. Likewise, DC-STAMP and macrophage fusion receptor (MFR) did not seem to regulate *Atp6v0d2* expression (Supplementary Figs. 4–6 online). However, mRNA levels of *Adam8* and *Adam12* in *Atp6v0d2*^{-/-} cells were markedly reduced (4–5 times) (Fig. 4c). Although ADAM8 and ADAM12 do not mediate fusion by themselves, they support osteoclast fusion *in vitro*^{16,17}. To examine whether increased ADAM8 or ADAM12 expression can rescue the fusion defect of *Atp6v0d2*^{-/-} osteoclasts, *Atp6v0d2*^{-/-} BMMs were transduced with either empty vector, ADAM8 retrovirus or ADAM12 retrovirus, and then subjected to osteoclast differentiation assays. Both ADAM8- and ADAM12-transduced *Atp6v0d2*^{-/-} BMMs generated significantly (*P* < 0.02) greater numbers of actin ring-positive, large TRAP⁺

macrophages was severely impaired in the absence of Atp6v0d2 (Supplementary Fig. 7). However, the involvement of Atp6v0d2 in cell-cell fusion is probably tissue specific, as *Atp6v0d2*^{-/-} mice do not show gross defects in other tissues or in the generation of offspring. Future studies should determine whether additional tissue-specific isoforms of the v-ATPase complex control cell-cell fusion processes. In addition to bone, these studies may provide important insights into the maintenance of other diverse physiological systems with prominent cell fusion processes, both in healthy and pathological conditions. The defect in osteoclast maturation observed in *Atp6v0d2*^{-/-} mice is very similar to that in mice deficient in DC-STAMP; however, *Atp6v0d2*^{-/-} mice also exhibit increased bone formation, suggesting that other cellular processes are altered.

Our study has potentially clinically important translational implications. The development of therapeutic agents, in particular for osteoporosis, that can prevent bone resorption while enhancing bone formation has long been desired. However, inhibition of osteoclasts also reduces or does not affect bone formation¹⁸. Hence, the likelihood of developing such therapeutics did not appear possible. However, our data regarding Atp6v0d2 provide strong genetic evidence in mice that such a therapeutic approach is theoretically attainable.

METHODS

Targeted disruption of the *Atp6v0d2* gene and mice. The targeting vector was constructed from the plasmid pPNT to replace the 330-bp fragment containing exon 1 (amino acids 1–43) of *Atp6v0d2* by standard procedures, essentially as described¹⁹. Flanking homologous genomic DNA was amplified from DNA of E14.1 embryonic stem (ES) cells by PCR. The linearized targeting constructs were electroporated into E14.1 ES cells, selected by G418 and gancyclovir, as described¹⁹. *Atp6v0d2*^{+/-} ES clones were identified by PCR and Southern blot analyses, and then injected into C57BL/6J blastocysts to yield chimeric mice that were subsequently crossed with C57BL/6 mice to yield *Atp6v0d2*^{+/-} mice. Mice were on a B6/129 background. *Tm7sf4* (the gene that encodes DC-STAMP)-deficient mice have been previously described³. All mouse work was performed under veterinary supervision in an accredited facility using protocols approved by the Animal Care and Use Committee of the University of Pennsylvania.

RNA and protein analysis. RNA was isolated using Trizol (Invitrogen) and subjected to northern blot analysis using either the 5'-terminal 440-bp fragment of the *Atp6v0d2* cDNA or the entire open reading frame of the *Atp6v0d1* cDNA. Real-time PCR was performed using the TaqMan universal PCR master mix on an ABI Prism 7000 Sequence Detection System (Applied Biosystems). Taqman primers for indicated genes were from Applied Biosystems. 250 ng of cDNA template generated using SuperScript II (Invitrogen) was used for each reaction. For western blot analysis, equal amounts of cell lysates were subjected to analysis with rabbit polyclonal Atp6v0d2-specific antibody or monoclonal antibody to Flag (Sigma), essentially as described¹¹. Rabbit Atp6v0d2-specific polyclonal antibodies were raised against Atp6v0d2 peptide (334–350 amino acids, used after purification on the affinity column containing the immunogenic peptide). Specificity was confirmed by the lack of cross-reaction to mouse Atp6v0d1 overexpressed in 293 cells.

Histological and morphometric analyses. Histology, μ CT imaging, and static and dynamic histomorphometry were carried out essentially as described (refs. 20,21 and Supplementary Methods online). Differences were considered significant at $P < 0.05$.

Osteoclast formation, F-actin staining and pit formation. Osteoclasts were prepared from bone marrow cells using two standard methods as described^{10,11}. TRAP assays, F-actin staining and pit formation were also carried out as described (refs. 10,11 and Supplementary Methods). To assess the resorption potential of osteoclasts derived from *Atp6v0d2*^{-/-} and wild-type mice, mean resorption area per osteoclast area and pit numbers on dentine slices

were determined as described²². The areas (in μm^2) of 60 individual TRAP⁺ MNCs, having an equal size and number of pits per group, were measured using the Via-160 video image maker measurement system (Boeckeler Instruments).

Retrovirus preparation and infection. Flag epitope-tagged cDNAs for Atp6v0d2, ADAM8 and ADAM12 were cloned into pMX-puro, transfected into PLAT-E cells to generate retroviruses that were used to infect BMMs as described¹¹. Briefly, BMMs were derived by culturing bone marrow cells (1×10^7 cells per dish) for 2 d in the presence of M-CSF (120 ng/ml), using Corning 100-mm suspension dishes (Corning Incorporated Life Science), and incubated with retroviruses in media containing M-CSF (120 ng/ml) and polybrene (5 $\mu\text{g}/\text{ml}$) for 6 h. After washing, BMMs were cultured overnight, detached with trypsin/EDTA and further cultured with M-CSF (120 ng/ml) and puromycin (2 $\mu\text{g}/\text{ml}$) for 2 d. Puromycin-resistant BMMs were induced to differentiate with M-CSF (30 ng/ml) and RANKL (150 ng/ml) for an additional 4–5 d.

Preparation of pre-osteoclasts and fusion. Preparation of mononuclear pre-osteoclasts and subsequent induction of fusion were performed, essentially as described¹³. Mononuclear pre-osteoclasts were prepared by coculturing BM cells (2×10^7 cells per dish) with calvarial osteoblasts (2×10^6 cells per dish) for 6 d in media supplemented with 10^{-8} M $1\alpha,25$ -dihydroxyvitamin D₃ ($1\alpha,25(\text{OH})_2\text{D}_3$) and 10^{-6} M prostaglandin E₂ (PGE₂). After removal of floating cells, mononuclear cells were harvested from attached cells by gentle pipetting. TRAP⁺ mononuclear pre-osteoclasts constituted more than 40–50% of the total cells harvested, and no multinucleated cells were detected. On the basis of alkaline phosphatase staining, no osteoblasts were detected. To induce fusion, purified mononuclear cells (1×10^5 cells per well, 200 μl per well, 96-well plates) were cultured with M-CSF (30 ng/ml) and RANKL (150 ng/ml) for 24 h. Cells were then stained for F-actin and TRAP, and bone resorption assays were performed as described above. When trans-well plates were used, F-actin and TRAP staining were performed on cells in lower wells, as osteoclasts are formed only in lower wells. For heterotypic fusion, pre-osteoclasts from wild-type and *Atp6v0d2*^{-/-} mice were incubated with the Vybrant cell-labeling dyes DiO and DiD (5 $\mu\text{g}/\text{ml}$, Molecular Probes), respectively, for 15 min. After washing, stained wild-type and mutant pre-osteoclasts were mixed in equal numbers and cultured on glass cover discs for 24 h under RANKL and M-CSF treatment. Cells were then examined using a Zeiss Axioplan II fluorescence microscope (Zeiss).

Statistical analysis. Data are expressed as mean \pm s.d or mean \pm s.e.m., as indicated, from at least three independent experiments for each experimental condition. Unless stated otherwise, statistical analysis was performed using the two-tailed Student's *t*-test to analyze differences between groups.

Note: Supplementary information is available on the Nature Medicine website.

ACKNOWLEDGMENTS

We thank the Abramson Family Cancer Research Institute Transgenic Core for ES cell injection. We also thank members of the Choi lab for discussion and reading of the manuscript, T. Kitamura (University of Tokyo) for pMX vectors and PLAT-E cells, D. Fremont (Washington University) for recombinant M-CSF, M. Takami (Showa University) for dentine slices, and D. Adams (University of Connecticut Health Center Image Core) for μ CT analysis. This work was supported in part by grants from the US National Institutes of Health (to Y.C., S.K.L., R.J.P. and J.A.L.).

COMPETING INTERESTS STATEMENT

The authors declare that they have no competing financial interests.

Published online at <http://www.nature.com/naturemedicine>
Reprints and permissions information is available online at <http://npg.nature.com/reprintsandpermissions/>

- Walsh, M.C. *et al.* Osteoimmunology: interplay between the immune system and bone metabolism. *Annu. Rev. Immunol.* **24**, 33–63 (2006).
- Teitelbaum, S.L. Bone resorption by osteoclasts. *Science* **289**, 1504–1508 (2000).
- Yagi, M. *et al.* DC-STAMP is essential for cell-cell fusion in osteoclasts and foreign body giant cells. *J. Exp. Med.* **202**, 345–351 (2005).

4. Nishi, T., Kawasaki-Nishi, S. & Forgac, M. Expression and function of the mouse V-ATPase d subunit isoforms. *J. Biol. Chem.* **278**, 46396–46402 (2003).
5. Sun-Wada, G.H., Yoshimizu, T., Imai-Senga, Y., Wada, Y. & Futai, M. Diversity of mouse proton-translocating ATPase: presence of multiple isoforms of the C, d and G subunits. *Gene* **302**, 147–153 (2003).
6. Smith, A.N., Borthwick, K.J. & Karet, F.E. Molecular cloning and characterization of novel tissue-specific isoforms of the human vacuolar H(+)ATPase C, G and d subunits, and their evaluation in autosomal recessive distal renal tubular acidosis. *Gene* **297**, 169–177 (2002).
7. Rho, J. *et al.* Gene expression profiling of osteoclast differentiation by combined suppression subtractive hybridization (SSH) and cDNA microarray analysis. *DNA Cell Biol.* **21**, 541–549 (2002).
8. Nishi, T. & Forgac, M. The vacuolar (H⁺)-ATPases—nature's most versatile proton pumps. *Nat. Rev. Mol. Cell Biol.* **3**, 94–103 (2002).
9. Stevens, T.H. & Forgac, M. Structure, function and regulation of the vacuolar (H⁺)-ATPase. *Annu. Rev. Cell Dev. Biol.* **13**, 779–808 (1997).
10. Suda, T., Jimi, E., Nakamura, I. & Takahashi, N. Role of 1 α ,25-dihydroxyvitamin D3 in osteoclast differentiation and function. *Methods Enzymol.* **282**, 223–235 (1997).
11. Kadono, Y. *et al.* Strength of TRAF6 signalling determines osteoclastogenesis. *EMBO Rep.* **6**, 171–176 (2005).
12. Li, Y.P., Chen, W., Liang, Y., Li, E. & Stashenko, P. Atp6i-deficient mice exhibit severe osteopetrosis due to loss of osteoclast-mediated extracellular acidification. *Nat. Genet.* **23**, 447–451 (1999).
13. Takami, M., Woo, J.T. & Nagai, K. Osteoblastic cells induce fusion and activation of osteoclasts through a mechanism independent of macrophage-colony-stimulating factor production. *Cell Tissue Res.* **298**, 327–334 (1999).
14. Chen, E.H. & Olson, E.N. Unveiling the mechanisms of cell-cell fusion. *Science* **308**, 369–373 (2005).
15. Verrier, S., Hogan, A., McKie, N. & Horton, M. ADAM gene expression and regulation during human osteoclast formation. *Bone* **35**, 34–46 (2004).
16. Abe, E., Mocharla, H., Yamate, T., Taguchi, Y. & Manolagas, S.C. Meltrin-alpha, a fusion protein involved in multinucleated giant cell and osteoclast formation. *Calcif. Tissue Int.* **64**, 508–515 (1999).
17. Choi, S.J., Han, J.H. & Roodman, G.D. ADAM8: a novel osteoclast stimulating factor. *J. Bone Miner. Res.* **16**, 814–822 (2001).
18. Martin, T.J. & Sims, N.A. Osteoclast-derived activity in the coupling of bone formation to resorption. *Trends Mol. Med.* **11**, 76–81 (2005).
19. Rho, J., Gong, S., Kim, N. & Choi, Y. TDAG51 is not essential for Fas/CD95 regulation and apoptosis *in vivo*. *Mol. Cell. Biol.* **21**, 8365–8370 (2001).
20. Lee, S.K. *et al.* Interleukin-7 influences osteoclast function *in vivo* but is not a critical factor in ovariectomy-induced bone loss. *J. Bone Miner. Res.* **21**, 695–702 (2006).
21. Montero, A. *et al.* Disruption of the fibroblast growth factor-2 gene results in decreased bone mass and bone formation. *J. Clin. Invest.* **105**, 1085–1093 (2000).
22. Jacquin, C., Gran, D.E., Lee, S.K., Lorenzo, J.A. & Aguila, H.L. Identification of multiple osteoclast precursor populations in murine bone marrow. *J. Bone Miner. Res.* **21**, 67–77 (2006).